D R A F T

The thermospheric response to geomagnetic storms

H. Lühr[1] and H. Liu[2]

[1] GeoForschungsZentrum Potsdam, Germany
[2] Div. of Earth and Planet. Science, Hokkaido University, Sapporo, Japan

Abstract. The dynamics of the upper atmosphere is strongly controlled by the intensity of the solar EUV radiation. This dependence is rather well described by models of the atmosphere, e.g. MSIS. On magnetically active days there are other sources of energy to the upper atmosphere, such as electric currents, which can surmount during storm days the effect of solar radiation. Due to high spatial and temporal variability of the geomagnetic input, the characterization of the thermospheric response is still quite vague. This situation is partly due to the lack of sufficient data. The low-altitude, polar orbiting CHAMP satellite provides with its high-sensitive accelerometer continuous measurements of thermospheric density and winds since August 2000. With the help of this unique data set, covering now half a solar cycle, the various aspects of the thermospheric dynamics can be studied in detail. We present recent findings of thermospheric dynamics based on CHAMP observations. For example, the degree of Joule heating depends not only on the current intensity, but also to a large extends on the dissipation efficiency. This has regional, local time and seasonal dependences. Only when taking these aspects into account, the storm-time thermospheric response can be interpreted correctly. For a few major storms in 2003 we present upper atmospheric features derived from CHAMP air drag and magnetic field measurements. The results are compared to model predictions.

Index Terms. Auroral currents, geomagnetic storm, thermospheric density, atmospheric model

1. Introduction

During geomagnetic storms the thermospheric density and composition experiences dramatic changes on global scale (e.g. Taeusch et al., 1971; Prölss, 1980, 1981; Forbes et al., 1996). The energy input is facilitated predominantly by field-aligned currents (FACs). The thermosphere responds to Joule/particle heating, Lorentz force (j x B), thermal up-welling and horizontal winds. Wave structures are identified as being able to distribute the disturbance (e.g. Williams et al., 1993; Forbes et al., 1995). On the other hand, Richmond (1979) reported that the propagation of thermospheric enhancements from high to low latitudes is mainly controlled by meridional winds.

It is expected that the thermosphere on the dayside responds differently during a storm than the night side. This point has been addressed in a simulation by Fuller-Rowell et al. (1994, 1996). One of their results is that the density enhancements at auroral latitudes propagate equatorward faster on the night than on the day side. Of interest are also the seasonal dependences. In a recent simulation Burns et al. (2004) found that the storm-time enhancement of the thermospheric temperature and composition is larger in winter than in summer. The authors attributed that to the relative importance of the storm-related heating with respect to the background solar heating. In the dark auroral region the solar heating is low therefore the storm-related Joule heating can be more important. Concerning the equatorward propagation of the disturbance, a larger velocity was predicted for the summer hemisphere since the background summer to winter circulation is adding here to the meridional disturbance winds (Fuller-Rowell et al., 1996).

With the satellite CHAMP we have the possibility to test a number of these hypotheses by observing the thermospheric dynamics at an altitude around 400 km. On its circular near-polar orbit it is covering all latitudes. A scan through all local times takes 130 days. The air drag experienced by the satellite is measured by a sensitive accelerometer. The readings of this instrument can be interpreted in terms of air density (Liu et al., 2005; Bruinsma et al., 2004). In a dedicated study Liu and Lühr (2005) have investigated the disturbances of the thermospheric density during the strong geomagnetic storms in Oct. and Nov. 2003. This study gives an impression of the diversity of effects in the thermosphere during storms.

In this paper we will shortly present the thermospheric density distribution during quiet times, discuss the roles of field-aligned current for the heating and finally concentrate on the response of the thermosphere during strong magnetic storms.

2. Data evaluation

Satellites traveling through the atmosphere experience a drag force in opposite direction to their motion. The acceleration, ***a***, caused by the drag is given by

$$\vec{a} = -\frac{1}{2}\rho\frac{C_d}{m}A_{eff}V^2\vec{v} \qquad (1)$$

where ρ is the thermospheric mass density, C_d the drag coefficient, m the satellite mass, A_{eff} the effective cross-section area, and V is the total velocity with respect to the air at rest, with $\vec{v}$ as the velocity unit vector in ram direction. The density can be estimated when solving Eq. (1) for ρ and inserting characteristic values for CHAMP. Further details of the applied approach to derive mass density from accelerometer measurements are given in Liu et al. (2005).

For comparison, density estimates based on the MSIS atmospheric model have also been calculated. The model was evaluated at the same position and time, using actual values for the activity parameters F10.7 and Ap .

In addition to the accelerometer CHAMP carries a suite of high-resolution magnetometers. These are used to estimate ionospheric currents. In particular, the auroral electrojets and the FACs are of interest in this context. The calculation approaches have been described elsewhere (Ritter et al., 2004; Wang et al., 2005).

3. General features of thermospheric density

Before starting with the disturbances caused by magnetic storms we want to introduce shortly the main characteristics of the thermosphere during quiet times, as observed by CHAMP. In a statistical study Liu et al. (2005) have investigated the mean density distribution at 400 km altitude for the year 2002. As can be seen from Figure 1, there is a density bulge on the dayside peaking around noon. This is evident both in the observations and in the predictions of the MSIS model.

Opposed to expectation maximum densities are not observed at the subsolar point but at mid-latitudes around ±30° magnetic latitude. This density feature, confined to the dayside, has rarely been reported before, and it is not included in the MSIS model. The fact that this double hump is well organized in magnetic coordinates is regarded as an indication that even the neutral atmosphere is strongly influenced by the magnetic field. This bifurcated density distribution resembles in some way the equatorial ionization anomaly of the F region plasma. Based on these observations, Liu et al. (2005) have suggested that in addition to ion drag, chemical heating in the E region may also play an important role in producing this anomalous structure in the distribution of the neutral density.

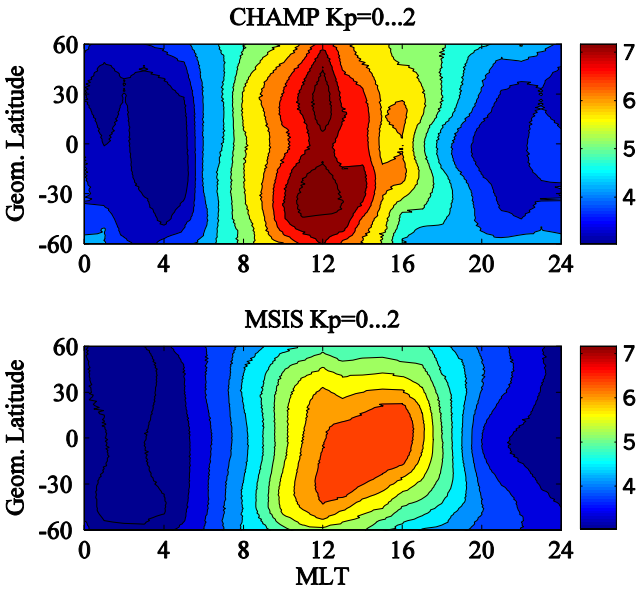

Fig. 1. Latitudinal distribution of the thermospheric mass density versus local time for quiet conditions (units: 10^{-12} kg/m³).

A further interesting feature, which is visible in Figure 1, is the pre-midnight enhancement. This so-called Midnight Density Maximum (MDM) has earlier been observed (Arduini et al., 1997) and was related to the Midnight Temperature Maximum (MTM) (Spencer et al., 1979).

Interesting new features also exist in the auroral regions. Here we expect the energy input from the solar wind-magnetosphere interaction. Average density distributions, as observed by CHAMP during quiet conditions in 2002, are shown in Fig. 2. Displayed is the relative difference between observation and the MSIS model in percent. Prominent density peaks in both hemispheres are observed between 70° and 80° mag. lat. around the noon sector. This area can be related to the cusp/cleft region. Already Lühr et al. (2004) had presented evidence for Joule heating in the cusp region, which subsequently caused the atmosphere to expand. They identified intense, small-scale FACs as the most probable cause for it. Another area of excess density is found in the midnight auroral region. This can be related to substorm activity. Obviously, the MSIS model does not account well for the additional heating sources such as field-aligned currents (FACs) and therefore underestimates the densities up to 30% in some regions. It is further interesting to note that other auroral regions such as the dawn/dusk flanks are not outstanding in density. It obviously requires a certain dissipation mechanism to make the heating through FACs efficient. First attempts to clarify that were made by Schlegel et al. (2005). They employed EISCAT radar measurements to probe the ionospheric conditions during times when CHAMP was passing by.

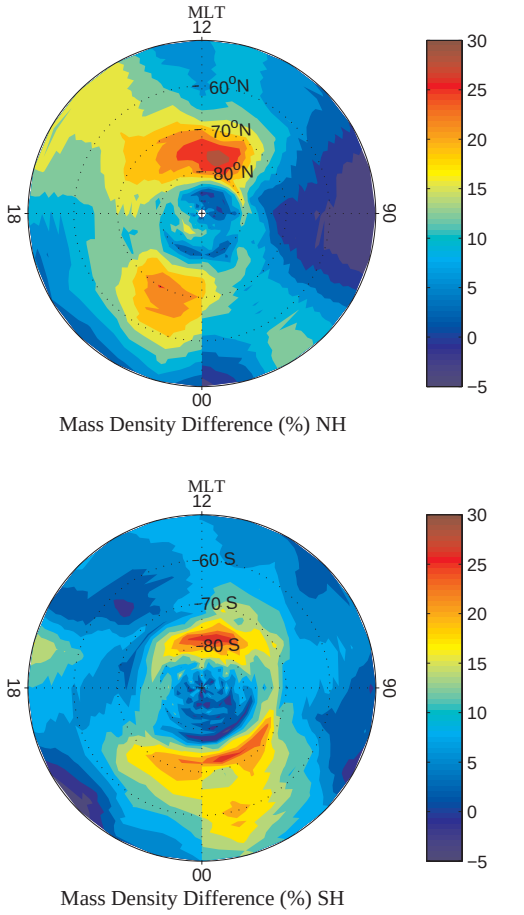

Fig. 2. Percentage difference of the thermospheric density between CHAMP and MSIS90 in the polar regions for quiet conditions (from Liu et al., 2005).

Keeping all these features of the quiet-time thermosphere in mind we will address the disturbances of the density caused by geomagnetic storms in the subsequent sections.

4. The thermosphere during magnetic storms

Geomagnetic storms are known to greatly affect the thermosphere. Direct evidence for that has earlier been deduced, for example, from the orbit perturbation of low-Earth orbiting satellites. Here we will present the perturbations in some details which were observed by the sensitive accelerometer on board the CHAMP satellite. As examples we have selected the two super storms in Oct. and Nov. 2003. These events are characterized by rather extreme conditions. D_{st} values as low as -401 nT were observed in Oct. and it went even down to -473 nT in case of the Nov. storm. Also the solar wind data were exceptional. The wind speed exceeded 1800 km/s in the Oct. event, and the IMF B_z component reached values below -50 nT in Nov. Further details of the exceptional geophysical conditions prevailing during these storms can be found in Gopalswamy et al. (2005) and references therein.

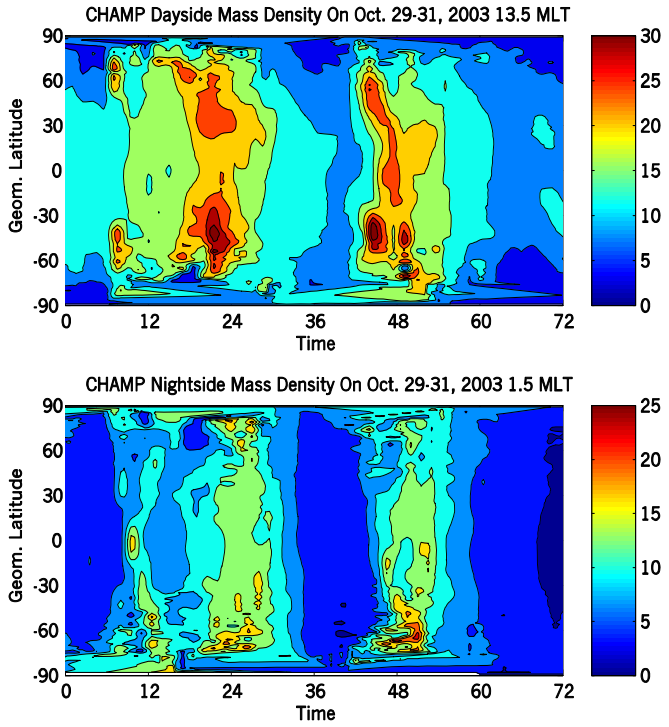

Fig. 3. Thermospheric density during the 29-31 Oct. 2003 magnetic storm. The upper panel shows the density sampled by CHAMP along the 1330 MLT meridian and the lower along 0130 MLT (from Liu and Lühr, 2005).

Thermospheric density responses to these severe storms have been studied in detail by Liu and Lühr (2005). Independent investigations of the Oct. storms were published by Sutton et al. (2005). During the period of interest in late 2003 the CHAMP orbital plane was close to noon/midnight. This fortunate constellation allowed us studying the effects on both the day and night side during each orbit. Figure 3 shows for the storm period 29-31 Oct. 2003 the succession of three storm phases. In the top panel density variations on the dayside are presented and below disturbances on the night side are shown. First enhancements show up at auroral regions on the dayside right after the SSC at 0611 UT, 29 Oct. No direct SSC-related signature is observed on the night side, except for a general density enhancement. About 3 hours after the SSC an equatorial midnight density maximum is occurring. This seems to be the source of a poleward propagating density wave. The second storm phase produces longer lasting density enhancements. They are observed first at auroral latitudes and then propagate to the dayside equator. The third storm phase exhibits quite similar features. Note, how far equatorward the density peaks occur during this event. It should be noted that we encounter here air densities up to 30×10^{-12} kg/m³, during quiet times it amounted to 7×10^{-12} kg/m³ on the dayside (cf. Fig. 1). On the night side the storm phases are also visible as density enhancements, but the amplitude is much lower, and the effect appears about two hours delayed compared to the dayside.

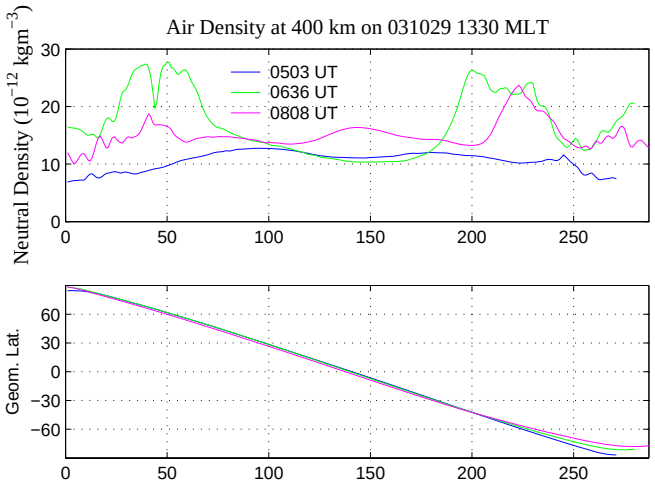

Fig. 4. Air density sampled by CHAMP traveling from north to south pole on the dayside. Readings are taken from three consecutive orbits. Start times of the tracks are given in the upper panel, time in units of 10 sec. First track occurs before the storm, the second starts 25 min after the SSC and the third starts two hours after SSC.

The density disturbances observed by CHAMP are caused by the combined effect of auroral zone heating and equatorial propagation. For the initial phase of the Oct. event three CHAMP dayside tracks are shown in Figure 4 occurring around the storm commencement (0611 UT). The first density profile from north to south (starting 0503 UT) occurs before the SSC and reflects the quiet-time thermosphere. The second pass starts 25 min after the SSC and encounters already huge density enhancements (factor of 3) in both auroral zones. The equatorial region is at this time (50 min after SSC) still unaffected. One and a half hour later the heating in the north hemisphere seems to have ceased, but now a density bulge has reached the equator. The southern auroral region is still active. Due to the combined effect of temporal and spatial variations it is difficult to clearly localize the heating region with a single satellite during active periods.

The density variations as predicted by the MSIS90 model are shown in Figure 5. Some enhancements are visible at the three storm phases. In general, there is, however, hardly any resemblance with the actual evolution of the density over three storm phases. Also the predicted amplitudes are signifantly too low. MSIS as an average model is not expected to reflect the conditions properly during severe conditions and can therefore not be recommended to be used for such extreme conditions.

The storm period in October consisted of a succession of three storms. The thermosphere probably did not have enough time between the phases to fully recover. Opposed to that the storm in Nov. is well isolated. Figure 6 shows the storm-time density variations. For a better visualization the quiet-time density distribution has been subtracted. Similar as in the previous event highest densities are encountered at auroral latitudes on the dayside. The effect is much more pronounced in the southern hemisphere and density peaks appear

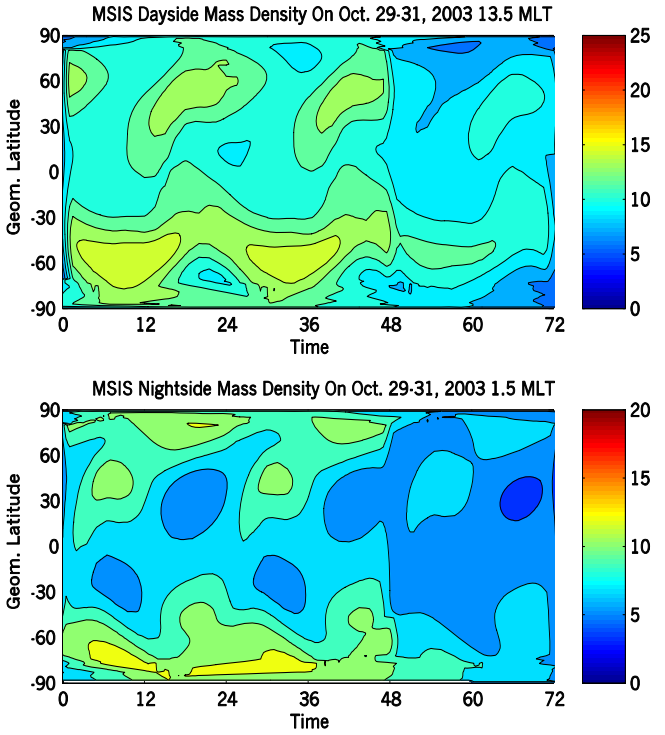

Fig. 5. The same as Fig. 3, but for predictions of the mass density from MSIS90.

significantly further equatorward displaced than in the north.

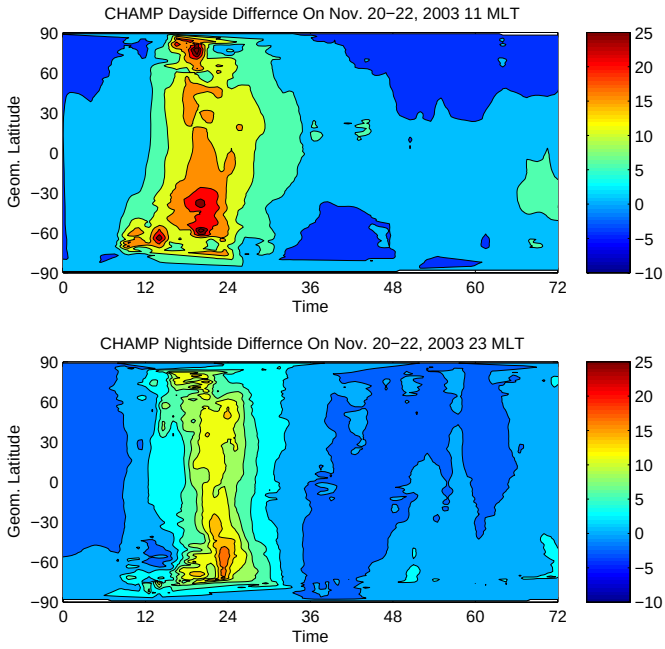

Fig. 6. Storm-time deviation of the thermospheric density during the 20-22 Nov. 2003 period (units: 10^{-12} kg/m³). Data in the upper and lower panel are sampled in the 11 and 23 MLT meridional plane, respectively.

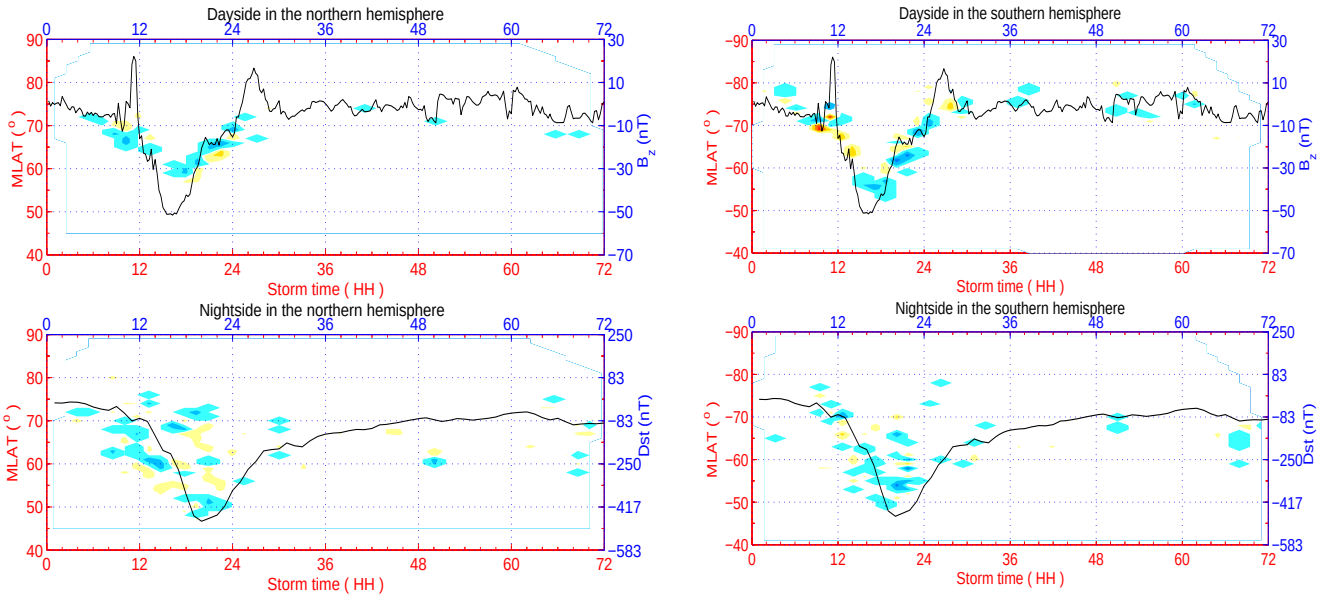

FIG. 7. Latitude variation of intense FACs on the dayside (top) and night side (bottem) at both auroral regions during the 20 Nov. 2003 storm. Blue dots mark downward flowing FACs and yellow/red upward FACs. The intensity scale ranges from dark blue = -10μA/m² to red = 10μA/m². Overlaid are the variation of the IMF BZ (top) and Dst (bottom) (from Wang et al., 2006).

The storm effect is also present on the night side but with a lower amplitude and again some two hours delayed. This storm occurs rather close to the Dec. solstice. We attribute therefore the hemisphere differences primarily to the seasonal effect. Higher heating rates seem to occur in the summer hemisphere both on the day and night sides.

As a prime cause for the density enhancement heating in the ionospheric E region is assumed. As a consequence of that the atmosphere expands and the outer layers become denser. It is common understanding that the storm-time thermospheric disturbances are due to Joule heating dissipation of the electric energy carried by Field-Aligned Currents (FAC). Large-scale FAC sheets (100 to 200 km thickness) are known to be well organized on average in region 1 and region 2 bands. In a dedicated study Wang et al. (2006) have investigated the characteristics of large-scale FACs , based on CHAMP observations, during the Oct. and Nov. 2003 storm periods. The results obtained there can be used for a direct comparison with the simultaneously observed density enhancements. Figure 7 shows the latitude distribution of the detected intense FACs for the Nov. event. Typical quiet time FACs with densities below 1 μA/m² have been omitted in order to highlight the storm effect. Blue points mark downward current, yellow/red dots upward currents. On the dayside there is a quite obvious equatorward expansion of the FACs footprints in both hemispheres during the course of the storm. In the southern hemisphere this reaches, however, to lower latitudes. Overlaid on this plot is the variation of the IMF B_z. This IMF component controls the latitudinal displacement of dayside auroral oval quiet closely. On the night side intense FACs are also observed. They expand in a similar way equatorward but fill, in contrast to the dayside, a wide latitudinal range between 50° and 75°. For comparison, here the D_{ST} variation is overlaid. The equatorward boundary seems to follow more closely the amplitude of this index. The lowest latitudes are reached in this time sector about two hours later than on the dayside.

When compared to the density distribution in Figure 6 we find on the dayside a general agreement between the peak locations of the two quantities. This includes the timing of the main phase, the enormous equatorward expansion of the active region and the delayed FAC activity on the night side. In detail it is, however, difficult to find any resemblance. Strongest FACs are rarely collocated with density peaks, nor is there a clear preference for upward or downward FAC of being responsible for the heating. The density peaks in the northern hemisphere appear significantly further poleward than the strong FACs. In the south the collocation of these two quantities is better fulfilled. On the night side the relation between FACs and density enhancement is even clear. Density enhancements are confined to auroral latitudes while FACs are observed down to 50° mag. Lat. From these discrepancies we may conclude that besides the FAC intensity there must be an additional quantity influencing the heating efficiency.

5. Discussion and conclusion

In the previous sections we have presented recent thermospheric density observations obtained by CHAMP. It shows that the air density distribution even on quiet days is not only controlled by the solar radiation but also significantly modified by the geomagnetic field geometry and its activity. These effects are insufficiently reflected in

atmospheric field models like MSIS, even for average conditions.

Concerning the storm-time thermospheric density disturbances, these are most pronounced in the dayside auroral regions. Since the enhancements appear first in these regions and have largest amplitudes there, it can be concluded that the prime storm-related heating is taking place there. This is, in principle, known for quite a while. Our observations show, however, that there is no simple power to current relation. Several additional factors seem to play a role in modifying the efficiency conversion. A prominent feature to note is that the hemispheric/seasonal asymmetry in the noon sector is different from that in the midnight sector during all the storms. In the noon sector, the density enhancement in the winter (northern) polar region occurred at somewhat higher latitudes than in the summer polar region. The average density enhancement in the summer (southern) hemisphere was larger and penetrated to lower latitudes than in the winter hemisphere. These features are consistent with the simulation results of Ful1er-Rowell et al. (1996).

On the nightside, a hemispheric/seasonal asymmetry between locations of the enhancement was not obvious in the polar regions. But it varied with individual events at middle and low latitudes. The density enhancement was stronger and penetrated to lower latitudes in summer than in winter during the last (Oct. 30--31) and the Nov. 20--21 storms. But the first storm (Oct. 29--30) showed on the night side the opposite feature. During this storm, the winter hemisphere experienced a much stronger disturbance than the summer hemisphere (see Figure 3). Therefore, the hemispheric/seasonal asymmetry of thermospheric density disturbances is obviously quite well organized on the dayside with larger amplitudes in the summer hemisphere but seem to vary from event to event, at least in the midnight sector. Here, the summer hemisphere does not always experience stronger disturbances than its winter counterpart. In general, our observations do not confirm the afore mentioned simulation results of Burns et al. (2004) predicting a stronger storm-time enhancement on the night side.

During magnetic storms the air density in the upper thermosphere is severely enhanced. From our observations we find, the typical life-time of such disturbances is of the order of 12 hours. This is primarily determined by the duration of energy input from the solar wind. The decay time after ceasing of the input is about 4 hours on the dayside and last some 2 hours longer on the night side. It is quite evident that the storm-related heating takes place in the auroral latitude. The disturbance is then propagating equator ward. FACs are assumed to transfer the energy into the high latitude region. This could be confirmed by a simultaneous investigation of the FAC distribution during the considered storms. On the dayside resulting density enhancements are much larger than on the night side even for equal FAC strengths. Also in the summer hemisphere the effect is stronger than in the winter hemisphere. All this suggest that the dissipation process is more efficient in the sunlit ionosphere than in the dark possibly due to the higher ionospheric conductivity.

Present day thermospheric models are not capable to describe appropriately the density response during magnetic storms. This is quite unfortunate because they are urgently needed for calculating and predicting the orbital evolution of low-Earth orbiting satellites. A more suitable parameterization of these models would require a better understanding of the heating mechanism and their dependence on various environmental influences.

We also looked into the equatorward propagation of the density disturbances. In the noon sector it is different from that in the midnight sector. Our cross-correlation revealed for the dayside a faster propagation in the summer hemisphere than in the winter hemisphere. This is consistent with the predictions of Fuller-Rowell et al. (1996). However, we also can show that the propagation on the dayside appears to be faster than on the night side. This contradicts the simulation results of the above cited study. They expect a prominent contribution of the large-scale circulation, which is directed poleward on the dayside and equatorward on the night side. A possible explanation of our observations is that the equatorward wind is mainly driven by the large storm-time density enhancement at auroral latitudes. Since this bulge is much larger on the dayside, also the wind speed should be higher here.

Investigations of the propagation effects are badly hampered by the spatial-temporal ambiguity of single satellite measurements. For the mitigation of this problem an appropriate model can be used for interpreting the readings. Unfortunately, no reliable models exist for storm-time conditions. The other possibility is to perform measurements simultaneously at several points in space. This more promising concept is adopted by ESA to be implemented in its Earth Observation Opportunity program. The selected mission *Swarm* is comprising of a fleet of three spacecraft and is carrying a complementary suit of instruments. For further details the relevant web sites should be visited http://www.esa.int/esaLP/ESA3QZJE43D_LPswarm_0.html Swarm is identified by ESA as European contribution to ILWS. On it low polar orbit it may help to solve many of the open issues in ionosphere, thermosphere research. In particular, it allows with its constellation of spacecraft to uniquely determine FAC densities, can distinguish between spatial and temporal variations of plasma and neutral air processes, and provides information from different altitudes and local times simultaneously. The design and fabrication phase has started late 2005 and the launch of the fleet is scheduled for early 2010.

References

Bruinsma, S., D. Tamagnan, and R. Biancale (2004), Atmospheric densities derived from CHAMP/STAR accelerometer observations, *Planet. Space Sci., 52*, 297-312.

Burns, A. G., T. Killeen, W. Wang, and R. G. Roble (2004), The solar-cycle-dependent response of the thermosphere to geomagnetic storms, *J. Atmos. Terr,. Phys., 66*, 1-14.

Forbes, J. M., F. A. Marcos, and F. Kamalabadi (1995), Wave structures in lower thermosphere density from satellite electrostatic triaxial accelerometer measurements, *J. Geophys. Res., 100*, 14.693-14.701.

Forbes, J. M., R. Gonzales, F. A. Marcos, D. Revelle, and H. Parish (1996), Magnetic storm response of lower thermospheric density, *J. Geophys. Res., 10*,, 2313-2319.

Fuller-Rowell, T. J., M. V. Codrescu, R. J. Moffett, and S. Quegan (1994), Response of the thermosphere and ionosphere to geomagnetic storms, *J. Geophys. Res., 99*, 3893-3914.

Fuller-Rowell, T. J., M. V. Codrescu, H. Rishbeth, R. J. Moffett, and S. Quegan (1996), On the seasonal response of the thermosphere and ionosphere to geomagnetic storms, *J. Geophys. Res., 101*, 2343-2353.

Gopalswamy, N., L. Barbieri, G. Lu, S. P. Plunkett, and R. M. Skoug, Introduction to the special section: violent sun-Earth connection events of October-November 2003, *Geophys. Res. Lett., 32*, doi: 10.1029/2005GL022 348, 2005a.

Liu, H., H. Lühr, V. Henize, and W. Köhler (2005), Global distribution of the thermospheric total mass density derived from CHAMP, *J. Geophys. Res., 110*, A04301; doi: 10.1029/2004JA010741.

Liu, H., H. Lühr (2005), Strong disturbance of the upper thermosphere density due to magnetic storms: CHAMP observations, *J. Geophys. Res., 110*, A09S29, doi: 10.1029/2004JA010908.

Lühr, H., M. Rother, W. Köhler, P. Ritter, L. Grunwaldt (2004), Thermospheric up-welling in the cusp region, evidence from CHAMP observations, *Geophys. Res. Lett., 31*, L06805, doi: 10.1029/2003GL019314.

Prölss, G. (1980), Magnetic storm associated perturbations of the upper atmosphere: recent results obtained by satellite-borne gas analyzers, *Rev. Geophys., 18*, 183-202.

Prölss, G. (1981), Latitudinal structure and extension of the polar atmospheric disturbance, *J. Geophys. Res., 86*, 2385-2396.

Richmond, A. D. (1979), Thermospheric heating in a magnetic storm: dynamic transport of energy from high to low latitudes, *J. Geophys. Res., 84*, 5259-5266.

Ritter, P., H. Lühr, A. Viljanen, O. Amm, A. Pulkkinen, and Sillanpää (2004), Ionospheric currents estimated simultaneously from CHAMP satellite and IMAGE ground-based magnetic field measurements: A statistical study at auroral latitudes, *Ann. Geophys., 22*, 417-430.

Schlegel, K, H. Lühr, J.-P. St.-Maurice, G. Crowley, and C. Hackert (2005), Thermospheric density structure over the polar regions observed with CHAMP, *Ann. Geophys., 23*, 1659-1672.

Sutton, E.K., J.M. Forbes, R.S. Nerem (2005), Global thermospheric neutral density and wind response to the severe 2003 geomagnetic storms from CHAMP accelerometer data, *J. Geophys. Res., 110*, A09S40, doi: 10.1029/2004JA010985.

Spencer, N. W., G. R. Carignan, H. G. Mayr, H. B. Niemann, R. F. Theis, and L. E. Wharton (1979), The midnight maximum in the Earth's equatorial thermosphere, *Geophys. Res. Lett., 6*, 444-446.

Taeusch, D. R., G. R. Carignan, and C. A. Reber (1971), Neutral composition variation above 400 kilometers during a magnetic storm, *J. Geophys. Res., 76*, 8318-8325.

Wang, H., H. Lühr, and S.-Y. Ma (2005), Solar zenith angle and merging electric field control of field-aligned currents: A statistical study of the southern hemisphere, *J. Geophys. Res., 11*, A03306, doi: 10.1029/2004JA010530.

Wang, H., H. Lühr, S.Y. Ma, J. Weygand, and R.M. Skoug (2006), Field-aligned currents observed by CHAMP during the intense 2003 geomagnetic storm events, *Ann. Geophys.*, 24, (in press).

Williams, P. J., S., T. S. Virdi, G. Owen, I. W. Mccrea, and K. S. C. Freeman (1993), Worldwide atmospheric gravity-wave study in the European sector 1985-1990, *J. Atmos. Terr. Phys., 55*, 683-696.